Journal Pre-proof

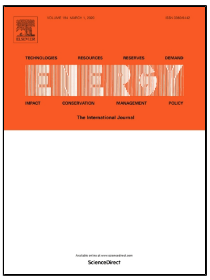

Effects of fluctuating thermal sources on a shell-and-tube latent thermal energy storage during charging process

Zhi Li, Xiaoli Yu, Lei Wang, Yiji Lu, Rui Huang, Jinwei Chang, Ruicheng Jiang

PII:	S0360-5442(20)30507-7
DOI:	https://doi.org/10.1016/j.energy.2020.117400
Reference:	EGY 117400
To appear in:	*Energy*
Received Date:	29 September 2019
Accepted Date:	14 March 2020

Please cite this article as: Zhi Li, Xiaoli Yu, Lei Wang, Yiji Lu, Rui Huang, Jinwei Chang, Ruicheng Jiang, Effects of fluctuating thermal sources on a shell-and-tube latent thermal energy storage during charging process, *Energy* (2020), https://doi.org/10.1016/j.energy.2020.117400

Effects of fluctuating thermal sources on a shell-and-tube latent thermal energy storage during charging process

Zhi Li [a,b,c], Xiaoli Yu [a,b], Lei Wang [b,d], Yiji Lu [a,c,*], Rui Huang [a,b,*], Jinwei Chang [a], Ruicheng Jiang [a]

[a] *Department of Energy Engineering, Zhejiang University, Hangzhou, 310027, China*

[b] *Ningbo Research Institute, Zhejiang University, Ningbo, 315100, China*

[c] *Durham Energy Institute, Durham University, Durham, DH1 3LE, United Kingdom*

[d] *Ningbo C.S.I Power & Machinery Group Co., Ltd., Ningbo, 315020, China*

H I G H L I G H T S

- Melting process of LTES under fluctuating thermal sources are analysed
- Fluctuating period and amplitude of fluctuating heat sources are investigated
- Large-period fluctuating heat sources significantly accelerate the meting process
- Melting rate increases but energy storage capacity decreases with amplitude rising
- Larger *Ste* reduces gap of melting rate between small and large period heat source

Abstract: The fluctuating and intermittent nature of industrial heat sources is a crucial technical barrier limiting the implementation of heat recovery energy systems. Latent Thermal Energy Storage (LTES) has the potential to overcome the issues maintaining the Waste Heat Recovery (WHR) system within the designed operational conditions for effective and efficient operation. However, the dynamic heat transfer characteristics of LTES under fluctuating heat sources need to be further

Email address: luyiji0620@gmail.com *(Y. Lu)*

hrss@zju.edu.cn *(R. Huang)*

studied to understand the effects of thermal fluctuation. In this work, charging performance of a shell-and-tube LTES under fluctuating and steady heat source has been investigated and compared. The effects of period and amplitude for the fluctuating heat source, as well as the Stefan number, are detailed investigated. Results indicate that large-period fluctuating heat sources can considerably reduce the total melting time but also the energy storage capacity, while small-period fluctuating heat sources almost has no effect on the melting process of LTES. For the effects of fluctuating amplitude, both the total melting time and energy storage capacity decline at a decreasing rate with the increase of fluctuating amplitude. The results can bridge the knowledge gap in the future designing of shell-and-tube LTES for fluctuating heat sources for the heat recovery applications.

Keywords: Thermal energy storage, Phase change material, Waste heat recovery, Fluctuating thermal source, Shell-and-tube heat exchanger

Nomenclature	
A	Fluctuating amplitude of heat source (K)
$c_{p,f}$	Specific capacity of heat transfer fluid (J/kg K)
$c_{p,p}$	Specific capacity of phase change material (J/kg K)
f	Liquid volume fraction
H	Total enthalpy of phase change material (J/kg)
h	Sensible heat of PCM (J/kg)
L	The latent heat of PCM (J/kg)
p	Pressure (Pa)
P	Fluctuating period of heat source (s)
ref	Reference state
r_i	Radium of inner tube (m)
r_o	Radium of outer tube (m)
T_{av}	Average temperature of heat source (K)
T_m	Melting temperature of PCM (K)
Greek letters	
α	Thermal expansion coefficient (K^{-1})
λ	Thermal conductivity (W/m K)
μ	Dynamic viscosity (Pa s)
ρ	Density (kg/m^3)
ε	Constant number

1. Introduction

Organic Rankine Cycle has been widely recognised as one of the most potential technologies to recover industrial waste heat, due to its high efficiency, high reliability and low cost [1, 2]. However, most of the available industrial heat sources possess fluctuating and intermittent nature, which is a crucial technical barrier limiting the implementation of ORC-based WHR systems [3]. The instability of industrial heat sources leads to ORC systems working under off-design conditions with low efficiency [4]. Latent Thermal Energy Storage (LTES) is a potential solution to buffer the fluctuation of industrial heat sources due to the high latent heat and constant phase change temperature [5, 6]. PCM-based thermal energy storage system absorbs heat from the waste heat source and then releases the stored heat to the WHR systems. Such systems have the superiority of overcoming the fluctuating of heat sources and maintaining ORC systems within design conditions.

A wide range of LTES using PCMs have been applied and studied in solar power plants and solar heating systems [7, 8]. For example, Li *et al.* [9] investigated the dynamic performance of a solar ORC system integrated with LTES considering solar disturbance. In the study, LTES is considered as a homogeneous heat capacity without considering the internal heat transfer process. Results showed that fluctuating period and amplitude of solar radiation affected the selection of optimal LTES volume and then influenced the ORC performance. Except for reducing the instability of solar radiation, LTES has also been applied to improve the matching performance of end-user demands in small-scale solar ORC systems and domestic-scale solar heating system. A representative work reported by Freeman *et al.* [10] from Imperial College London discussed the different thermal energy storage solutions for a domestic-scale solar CHP system to meet the heat and electricity demand in the night.

The authors focused on the energy storage performance of LTES without considering its heat transfer performance under dynamic inlet parameters. The resulted demonstrated the importance of LTES design on system performance. However, due to the variation of solar radiation in large time scale and demand in energy storage, most of the studies generally neglected the effects of fluctuation of solar radiation on the heat transfer performance of LTES and paid more attention to the system operating performance and the design/optimisation of LTES.

In the application for industrial waste heat recovery, LTES also plays an important role to bridge the gap between the heat sources and heat recover energy systems. Fabio *et al.* [11] proposed a PCM-coupled steam generator for dynamic industrial waste heat recovery. In this study, the PCM was simplified as big heat capacity and the results indicated that the PCM-based system could significantly reduce the thermal power fluctuating of the heat source and enlarge the high-efficiency working zone. Yu *et al.* [12] designed an ORC system using the concept of double shell-and-tube LTES. This study considered the effects of PCM thermophysical properties and LTES volume on the performance of the proposed ORC system to recover fluctuating thermal energy. The results showed the superiority of PCM-based combination system for fluctuating heat source without considering the detailed heat transfer process within the LTES. Xu *et al.* [13] concluded a forward-looking perspective about time-dependent waste heat recovery that thermal energy storage could address the time matching, spatial matching and energy grade matching between the energy source and demand, which is promising to be used as a next-generation heat recovery technologies.

Since the thermal behaviours of PCM have a great influence on the charging-discharging process of LTES, reported numerical and experimental researches have focused on the heat transfer

characteristics of the LTES systems under steady boundary conditions. Some studies investigated the effects of geometrical and thermophysical parameters and thermal boundary conditions on the melting process. Guo *et al.* [14] performed a numerical study to assess the effects of heat exchanger geometry and thermal boundary conditions on the energy storage performance of a vertical shell-and-tube LTES. Wang *et al.* [15] studied the effects of the temperature difference between the Heat Transfer Fluid (HTF) and the melting point of PCM, as well as the inlet mass flow rate on the charging performance of a horizontal shell-and-tube LTES. Tao *et al.* [16] evaluated the effects of the PCM thermophysical properties on the charging performance of a high-temperature LTES unit. Other studies have concentrated on the heat transfer enhancement and heat exchanger design of LTES systems. Francis *et al.* [17] compared the melting process of three LTES systems with circular and longitude fins and without fins. Wang *et al.* [18] carried out a numerical study to analyse the meting process of shell-and-tube LTES under different geometrical parameters of fins, including fin length, fin ratio and fin angle. Heat pipes [19], nanoscale additives [20], porous media [21] and cascaded PCM [22] were also used to enhance the heat transfer performance of shell-and-tube LTES systems. The design of LTES heat exchangers has also attracted much attention in recent years. The design of LTES heat exchangers also has been paid much attention as reported in recent studies. For example, Fang *et al.* [23] developed an analytical method to design the required heat transfer length and predict the energy storage ratio based on the effectiveness-NTU theory for any tube-in-tank LTES systems. Deng *et al.* [24] performed a numerical study to find out the optimal layouts of fins for a shell-and-tube latent LTES.

However, the majority researches on shell-and-tube LTES systems are performed based on steady

thermal boundary conditions. When the unsteady heat source was considered, the detailed heat transfer process of PCM under fluctuating thermal boundaries is less considered in the previously reported studies. The most of related studies conducted calculations by thermodynamic analysis or considering the PCM as large heat capacity. However, the fluctuation in inlet temperature or mass flowrate shown in **Fig. 1** should be considered in the design stage of LTES systems for industrial waste heat recovery. Because the characteristics of industrial heat sources including the period and amplitude are quite different from that of solar radiation, leading to different heat transfer and energy storage performance between the LTES systems designed based on steady and unsteady inlet parameters. Some researchers have noticed this challenge. In a pioneer work, Tao *et al.* [25] numerically studied the charging performance of a shell-and-tube LTES under unsteady inlet temperature and mass flow rate with a linear variation. The results indicated that the larger initial inlet temperature and mass flow rate could substantially reduce the melting time of the paraffin LTES. Elbahjaoui *et al.* [26] evaluated the effects of laminar fluid flow with pulsed inlet pressure on the melting process of a shell-and-tube LTES unit. The numerical results showed that the inlet pressure of the laminar flow with low pulsating frequency and high pulsating amplitude could reduce the total melting time. Xu *et al.* [27] optimised the thermal performance of a cascaded shell-and-tube LTES system with a quadratic-variation inlet temperature of HTF from the aspect of exergy, entropy and entransy analysis. The optimised results showed that the optimal thermal performance of steady case was better than that of the fluctuating case. To increase the energy storage density and reduce the final average temperature of a solar LTES tank, Huo *et al.* [28] investigated the effects of the time-dependent intermittent heat flux on the energy storage performance. The proposed transient heat

flux has the characteristic of square wave and its period and amplification were numerically evaluated. The results proved that the time-dependent heat flux could reduce the final average temperature but increase the total melting time compared to the constant heat flux.

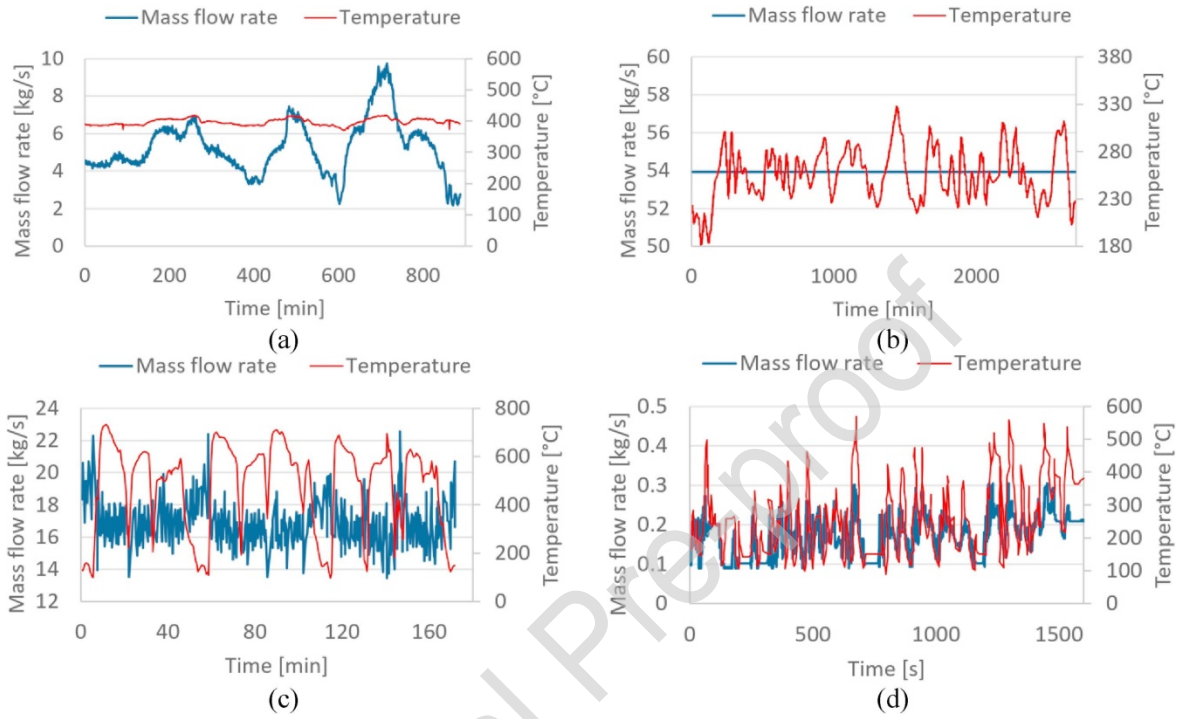

Fig. 1. Fluctuating characteristics of different waste heat source: (a) Steel billet reheating furnace; (b) Clinker cooling; (c) Electric arc furnace; (d) Internal combustion engine exhaust [29].

Based on the above literature study, it can be found that the heat transfer process of a shell-and-tube LTES under sinusoidal inlet temperature has not been considered previously. Furthermore, the effects of different amplitudes, especially the periods to simulate different real industrial heat source shown in **Fig. 1** for sinusoidal heat sources should be revealed. Therefore, in this study, the heat transfer process and energy storage performance of a shell-and-tube LTES heated by sinusoidal inlet temperature are investigated. In detail, the effects of different period and amplitude, as well as the Stefan number are analysed based on CFD simulations. The completion of this work can contribute to

the understanding of heat transfer process of shell-and-tube LTES under fluctuating thermal boundaries, as well as the design and optimisation of LTES unit integrating with ORC-based WHR systems for industrial waste heat recovery.

2. Description of the simulation model

2.1 Physical model

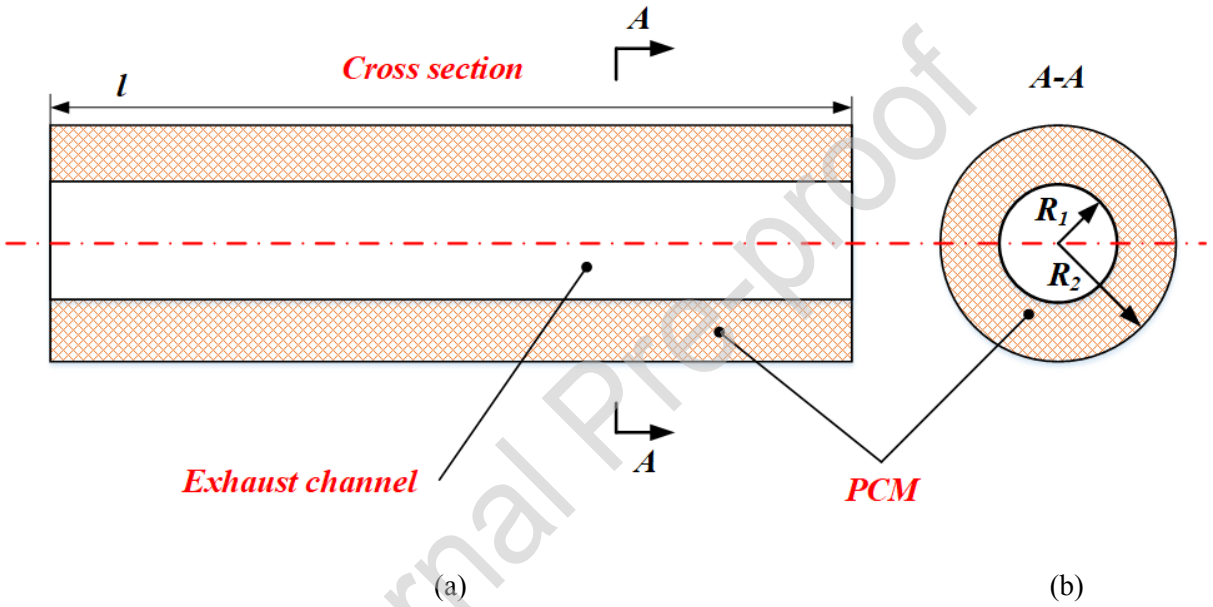

Fig. 2. Sketch of the shell-and-tube latent thermal energy storage evaporator

(a) Front view in section, (b) Cross-sectional view

The heat exchanger as illustrated in Fig. 2 is a typical cylindrical shell-and-tube LTES heat exchanger. The PCM is placed in the shell side while HTF flows through the tube side. The layout can maximise the heat transfer area of exhaust gas and PCM, as well as bear high-pressure fluid. The length of the LTES heat exchanger is 1000 mm, and the radius for the inner tube and outer shell are 12.5 mm and 25 mm respectively. Along the flowing direction of HTF, each cross-section of PCM is heated by the fluctuating heat source and they undergo similar heat transfer process. Therefore, a two-dimensional

cross-section at the inlet of LTES has been selected as the physical model. Before establishing the mathematical model, the following assumptions are adopted to simplify the physical model and later computation.

(1) The thermophysical properties of PCM are independent with temperature.

(2) The flow in the liquid PCM is assumed to be Newtonian laminar and incompressible.

(3) The thermal resistance of the inner wall is neglected while the outer wall of the LTES is adiabatic.

The thermophysical properties of the selected PCM are listed in **Table 1**.

Table 1 Thermophysical properties of the selected PCM

Parameters	PCM ($LiNO_3$-$NaNO_3$-KCl) [30]
ρ (kg/s)	2297
λ (W/m K)	0.88
c_p (J/kg K)	1330
μ (Pa s)	0.003
T_m (K)	433
ΔH (kJ/kg)	266
α (K^{-1})	0.0004

2.2 Governing equations

In this section, a two-dimensional transient heat transfer model for the cross-section of LTES based on the enthalpy method is presented to simulate the moving boundary problem within the PCM. The

continuity equation for PCM is written as follows

$$\frac{\partial \rho}{\partial t}+\frac{\partial(\rho u)}{\partial x}+\frac{\partial(\rho v)}{\partial y}=0 \tag{1}$$

In the enthalpy method, the energy equations for liquid state and solid state have the same form. The solid-liquid interface is indicated as a mushy zone to separate two phases. The energy equation for PCM is described as follows:

$$\frac{\partial \rho H}{\partial t}+\frac{\partial(\rho u H)}{\partial x}+\frac{\partial(\rho v H)}{\partial y}=\frac{\partial}{\partial x}\left(k\frac{\partial T}{\partial x}\right)+\frac{\partial}{\partial y}\left(k\frac{\partial T}{\partial y}\right) \tag{2}$$

Where H represents the total enthalpy of sensible enthalpy and latent enthalpy, which can be calculated by equation (3) and (4). h_{ref} denotes the sensible enthalpy at the reference temperature T_{ref}.

$$H=h+f\cdot L \tag{3}$$

$$h=h_{ref}+\int_{T_{ref}}^{T}c_p dT \tag{4}$$

Where f refers to the liquid volume fraction calculated by equation (5). It should be pointed out that the liquid volume fraction lies between 0~1 in the mushy zone.

$$f=\begin{cases}0 & T<T_{solidus}\\ \dfrac{T-T_{solidus}}{T_{liquidus}-T_{solidus}} & T_{solidus}\le T\le T_{liquidus}\\ f=1 & T>T_{liquidus}\end{cases} \tag{5}$$

Substituting equation (3)-(5) into equation (2), the energy equation can be further written as

$$\frac{\partial \rho h}{\partial t}+\nabla\cdot(\rho v h)=\nabla\cdot(k\nabla T)-\frac{\partial \rho f L}{\partial t}-\nabla\cdot(\rho v f L) \tag{6}$$

The natural convection has significant improvement in accelerating the melting process of LTES [31].

Due to the small variation in density, the natural convection is taken into consideration via the Boussinesq approximation [32]:

$$\left(\rho-\rho_0\right)g=-\rho_0\beta\left(T-T_0\right) \tag{7}$$

Then the momentum equation considering natural convection for PCM has a form as follows:

$$\frac{\partial\left(\rho u\right)}{\partial t}+\frac{\partial\left(\rho uu\right)}{\partial x}+\frac{\partial\left(\rho uv\right)}{\partial x}=-\frac{\partial p}{\partial x}+\frac{\partial}{\partial x}\left(\mu\frac{\partial u}{\partial x}\right)+\frac{\partial}{\partial y}\left(\mu\frac{\partial u}{\partial y}\right)+A_{mush}u \tag{8}$$

$$\frac{\partial\left(\rho v\right)}{\partial t}+\frac{\partial\left(\rho uv\right)}{\partial x}+\frac{\partial\left(\rho vv\right)}{\partial x}=-\frac{\partial p}{\partial y}+\frac{\partial}{\partial x}\left(\mu\frac{\partial v}{\partial x}\right)+\frac{\partial}{\partial y}\left(\mu\frac{\partial v}{\partial y}\right)+A_{mush}v+\rho g\alpha\left(T-T_m\right) \tag{9}$$

In equation (9), the parameter A_{mush} is a constant to describe how fast the velocity is decreased to zero when the PCM solidifies, which is calculated by [33]:

$$A_{mush}=-C\frac{\left(1-f\right)^2}{f^3+\varepsilon} \tag{10}$$

The constant ε is a very small number to prevent the division by zero.

2.3 Model of fluctuating heat source

As depicted in **Fig. 1**, the temperature of different heat sources can fluctuate in different periods varying from minutes even seconds to hours, as well as in different amplitudes. The fluctuating period and amplitude are important indicators to represent the characteristics of fluctuating different heat sources. To reveal how fluctuating heat sources affect the heat transfer process of the latent thermal energy storage, the effects of fluctuating periods and amplitudes for fluctuating heat sources need to be investigated. In this study, the inlet temperature of the fluctuating heat source is assumed as a sinusoidal function in the following equation:

$$T_{HTF}=a\cdot\sin(\pi t/b)+573 \tag{11}$$

When the effects of different periods and amplitudes are studied, the values of coefficients in formula (11) are listed in **Table 2** and **Table 3**, respectively. It should be pointed out that the average temperature of different fluctuating heat sources is fixed at 573 K in an hour.

Table 2 Coefficient values of inlet temperature with different periods.

Cases	**a**	**b**
P=1 min	100	30
P=2 min	100	60
P=6 min	100	180
P=20 min	100	600
P=30 min	100	900
P=60 min	100	1800

Table 3 Coefficient values of inlet temperature with different amplitudes.

Cases	**a**	**b**
A=50 K	50	1800
A=75 K	75	1800
A=100 K	100	1800
A=125 K	125	1800
A=150 K	150	1800

2.4 Initial and boundary conditions

The initial conditions for PCM

$$T_{PCM}\left(x,y\right)=T_m-10 \tag{12}$$

The boundary condition for HTF is

$$T_{HTF,in}=T_{HTF} \tag{13}$$

The boundary condition for the outer wall is

$$\frac{\partial T_{PCM}}{\partial r}\left(r=r_2\right)=0 \tag{14}$$

The boundary condition for the inner wall is

$$h_{HTF}\left(T_{HTF}-T_{PCM}\right)=-k\frac{\partial T_{PCM}}{\partial r}\left(r=r_1\right) \tag{15}$$

3. Independency study and model validation

The computation is conducted in the software Ansys/Fluent 14.5. Before the simulation, the verification of grid size and time step are conducted. The computational domain is a two-dimensional annulus. The grid is created in three different sizes of 0.5 mm, 0.8 mm and 1 mm, corresponding to the grid number of 6006, 2384 and 1580. Meanwhile, four different time steps including 0.5 s, 1 s, 2 s and 5 s are also studied to demonstrate the selected time step does not affect the computational results. **Fig. 3** shows the results of the verification of the time step and grid size. According to the verification results, the grid size of 0.8 mm (grid number of 2384) and a time step of 2 s are selected in the simulation model.

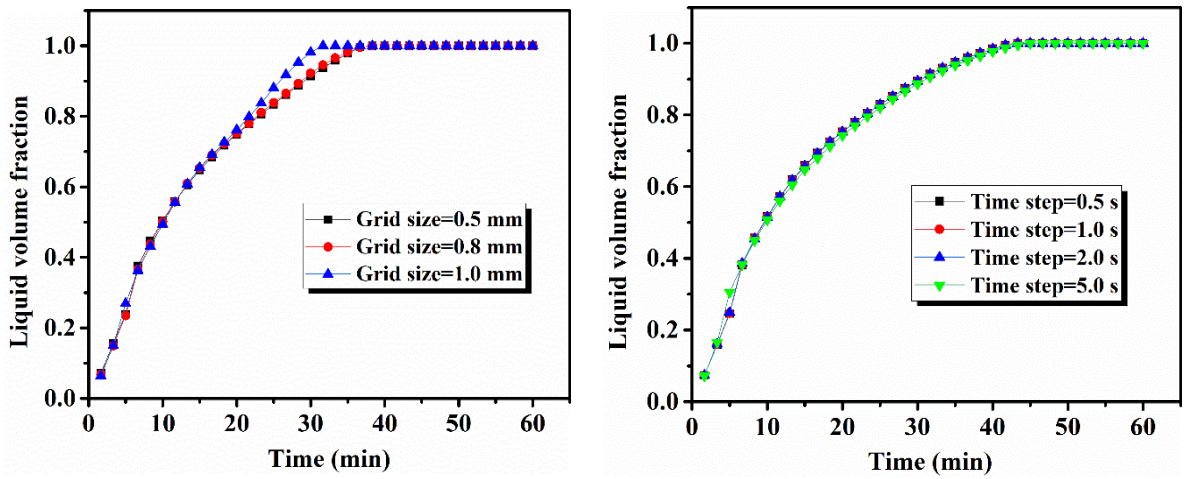

Fig. 3. Validation of the computational time step and grid size: (a) grid size; (b) time step.

A comparison between the present simulation and experimental results from reference [34] has been conducted to validate the numerical model. The comparative results are illustrated in **Fig. 4**. The reported temperature in the present simulation fits well with the experimental data in reference [34]. The error analysis indicated the maximum error between the present simulation results and experimental date in reference [34] is 4.67 %, which proves the reliability and correction of the adopted numerical model.

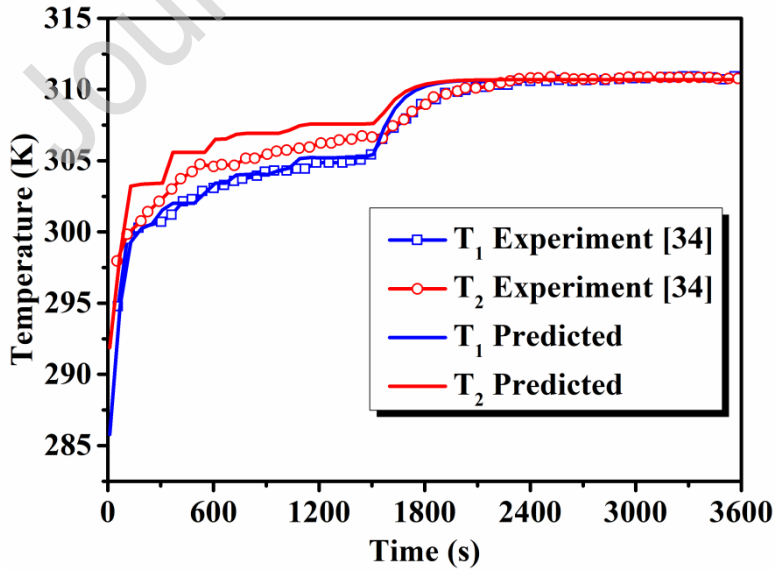

Fig. 4. The comparison between the present simulation and experimental results from reference [34].

4. Results and discussion

4.1 Effects of fluctuating period

Fig. 5 shows the timewise liquid volume fraction of PCM heated by heat sources with different period. Because the fluctuating heat source is modelled as a sinusoidal function in the study, it can be known that the temperature of fluctuating heat source in every first-half period is higher than that of every second-half period in a whole period, which indicated the PCM could absorb more heat from the fluctuating heat source during the every first-half period than that of every second-half period. That is the reason to explain the liquid volume fraction increases fast in the first half period and then increases with a much slower rate in the second half period for fluctuating heat sources, i.e., the evolution of liquid volume fraction presents a wavelike (like a wavy line) rise trend as shown in **Fig. 5**. Taking the case of P=20 min as an example, it can be found that the liquid volume fraction shows different increasing rate during the first and second half period in a whole period. In detail, the liquid volume fraction of P=20 increases fast in the time-lag of 0~10 min, but it increases with a much lower rate in the time-lag of 10~20 min. The evolution trend of liquid volume fraction is similar to that of time-lag of 20~40 min. It can be found that the wavelike rise trend is more significant for fluctuating heat sources with a larger period (P=20 min, 30 min, 60 min) rather than cases with a smaller period (P=1 min, 2 min, 6 min). The reason is that the difference of the heat transferred from HTF to PCM between the first and second half period is small for small-period fluctuating heat sources, while the difference is large for large-period cases during a whole period.

Compared to the constant heat source, it can also be found that the fluctuating heat sources with

smaller period (P=1 min, 2 min, 6 min) have little effects on the evolution of liquid volume fraction, while the large-period (P=20 min, 30 min, 60 min) fluctuating heat sources can accelerate the melting process, especially in the early stage (t<20 min). In detail, the liquid volume fraction under small-period fluctuating heat sources have a minor enhancement of liquid volume fraction in the early stage, but the improvement effects keep decreasing later and finally, they only shorten the complete melting time of PCM to a very small extent. For large-period fluctuating heat sources, although the enhancement effects decrease after the early stage, they still cut down the total melting time to some extent according to the scale of the fluctuating period.

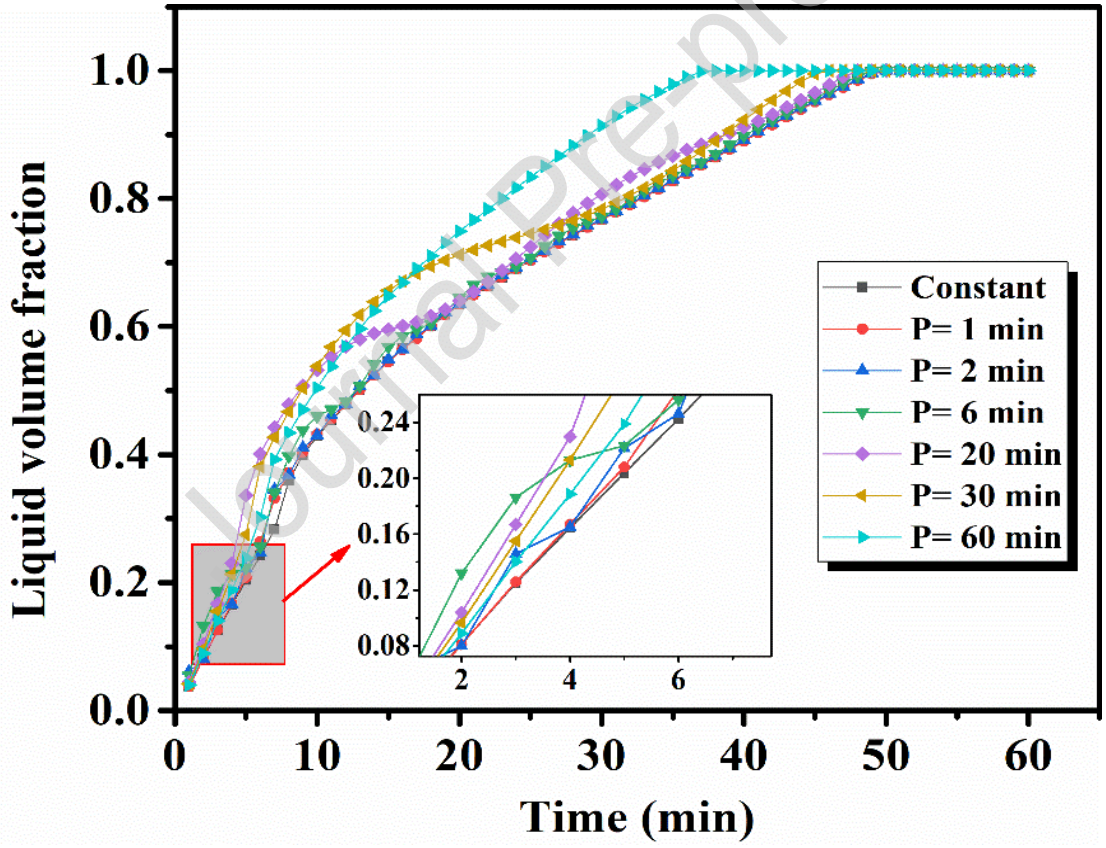

Fig. 5. The evolution of liquid volume fraction with melting time under different heat sources.

The total melting time for different heat sources is presented in **Fig. 6**. The values for small-period (P=1 min, 2 min, 6 min) fluctuating heat sources are 49.8 min, 49.7 min and 49.3 min, respectively,

which are almost the same as the constant heat source (49.7 min). However, the total melting time decreases distinctly with the increase of the period for large-period (P=20 min, 30 min, 60 min) fluctuating heat sources, especially the total melting time (37.3 min) for the period of P=60 min is around 25% shorter than that of the constant heat source.

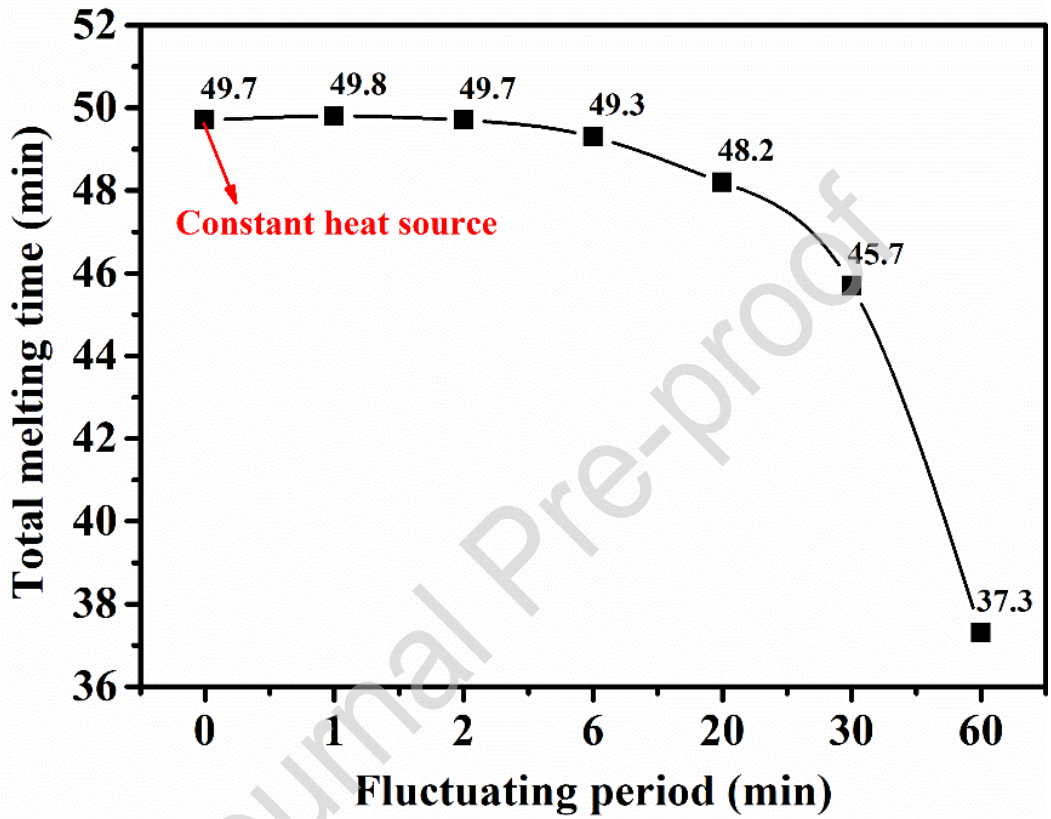

Fig. 6. The total melting time for fluctuating heat sources with different period.

The evolution of liquid volume fraction is related to the timewise heat flux transferred from HTF to PCM shown in **Fig. 7**. Taking the heat flux of the constant heat source as the baseline, it can be found that the heat flux of fluctuating heat sources fluctuates up and down the baseline with the approximate symmetry. For constant heat source, the heat flux gradually decreases with time because of the rise of the average PCM temperature. Regarding to fluctuating heat sources, the heat flux presents wavelike characteristics corresponding to the periodic variation of HTF temperature. For small-period

fluctuating heat sources, the total heat flux varies in a large range with high frequency in every period, leading to the heat stored by PCM in a period very closed to that of the constant heat source in the same time-lag, and this is the reason to explain the little difference in the evolution of liquid volume fraction between the fluctuating and constant heat sources. Nevertheless, that is not the case for large-period fluctuating heat sources.

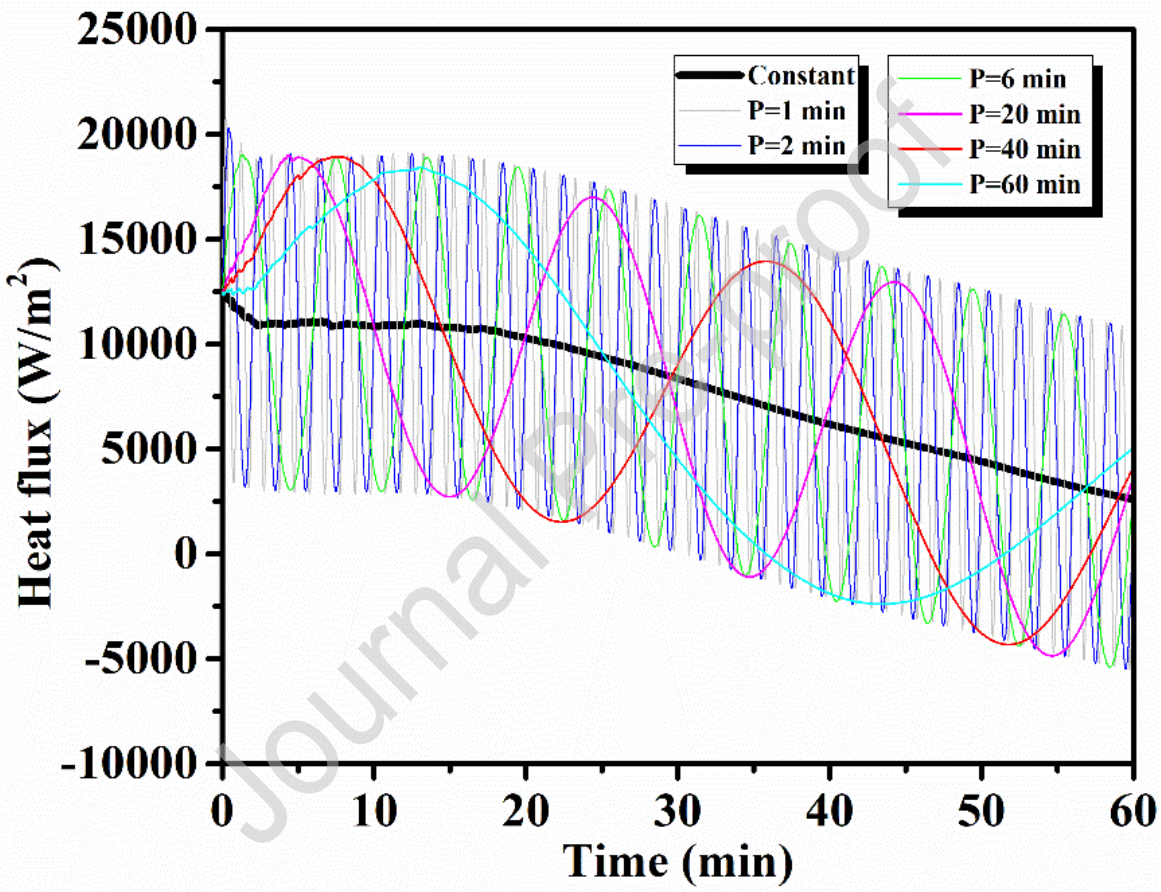

Fig. 7. The timewise heat flux for fluctuating heat sources with different period.

Fig. 8 demonstrates the heat absorbed by PCM in each unit time (1 minute). It can be seen that the heat absorbed by PCM in every minute for the case of P=1 min completely coincides with that of the constant heat source, resulting in their similar evolution of liquid volume fraction, i.e., almost the same melting process. For the case of P=2 min and P=6 min, it can be known that the total heat

absorbed by PCM in a corresponding period has little difference with that of constant heat source in the same time-lag during the whole melting process, due to the symmetrical shape of total heat absorbed by PCM up and down the baseline in every corresponding time-lag. Especially in the earlier stage of the melting process (t<10 min), almost equal amount of heat transferred to the PCM cannot lead to significant natural convection in the liquid PCM due to the small liquid volume fraction for both the constant heat source and fluctuating heat sources, and the heat transfer process is dominated by heat conduction, as a result, the fluctuating heat sources with small period make little effects on the evolution of liquid volume fraction. However, for large-period fluctuating heat sources, the total heat absorbed by the PCM is quite larger than that of the constant heat sources in the earlier stage of the melting process (t<10 min), which significantly enhances the heat transfer process of PCM and lead to large liquid volume fraction. In return, the natural convection existing in the liquid PCM improves the heat transfer rate between the HTF and PCM. As shown in **Fig. 5**, that is the reason to explain the distinctly faster melting process of PCM for the large-period fluctuating heat sources compared with the constant heat source and small-period fluctuating heat sources in the early stage (t<20 min).

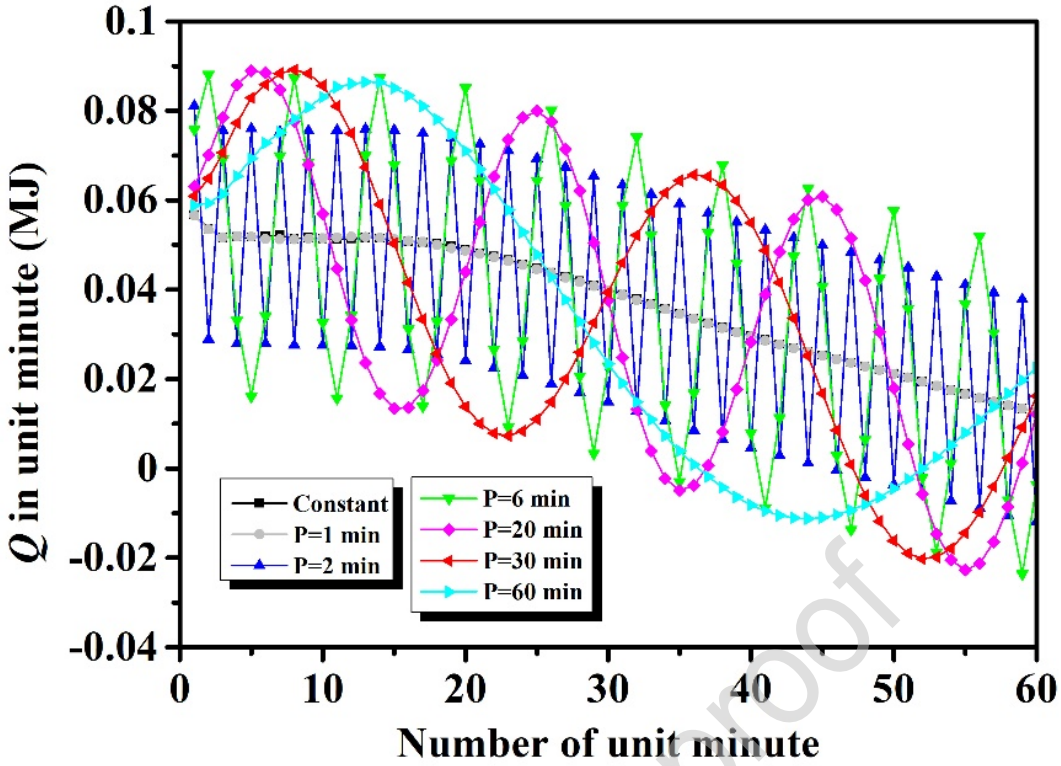

Fig. 8. The heat absorbed by PCM under different fluctuating heat sources in each unit time.

To further interpret the phenomenon, the temperature distribution and solid-liquid interface of PCM for different heat sources at different moments are presented in **Fig. 9**. The left semicircle is the temperature contour while the right one is the solid-liquid interface. Taking the results of constant heat source as the comparison, the moments at t=300 s, t=550 s, t=1100 s and t=2000 s are corresponding to the moments of liquid volume fraction f=0.2, f=0.4, f=0.6 and f=0.8, respectively. It is apparent that the case of P=20 min showsthe fastest meting process of PCM, while the case of P=30 min and P=60 min have minor effects to enhance the melting process at the moment of t=300 s, and the PCM average temperature of these cases shown in **Fig. 9** is significantly higher than that of constant heat source and small-period fluctuating heat sources. Whether the liquid volume fraction or the temperature contour of PCM, there is little difference between the small-period fluctuating heat sources and constant heat sources at the moment of t=300 s. As the previous analysis of **Fig. 8**, the

reason is related to the total heat transferred to PCM in a time-lag. The total heat absorbed by PCM for small-period fluctuating heat sources (P= 1min, 2 min, 6 min) is almost the same as the constant heat source in the early stage of melting process, even the whole melting process, bringing about little difference in the evolution of liquid volume fraction and contour temperature. However, the large-period fluctuating heat sources can transfer much more heat to the PCM during the earlier stage (t<10 min), even the early stage (t<20 min) of the melting process, therefore, the liquid volume fraction rises rapidly and natural convection occurring in the liquid PCM improves the meting rate in turn. For example, in the first 5 minutes of the melting process, the case of P=20 min transfers the most heat to the PCM, leading to the highest average temperature and liquid volume fraction of PCM among all the heat sources shown in **Fig. 9**.

In later moments, it can be found that the difference in the solid-liquid interface and temperature distribution of PCM still keeps unapparent between the small-period fluctuating heat sources and constant heat source, owing to the similar amount of heat transferred to PCM during every corresponding time-lag. That can explain the narrow margin in the evolution of liquid volume fraction for the small-period fluctuating heat sources and constant heat source. However, for the large-period fluctuating heat sources, various degrees of enhancement effects are observed corresponding to different period compared with the constant heat source. The larger the fluctuating period, the more substantial the enhancement effects can be observed. That is relevant to the scale of the period. For the case of P=20 min and P=30 min, their timewise heat flux in the latter half period is quite smaller than that of the former half period in a whole period, which is also smaller than that of the constant heat source in the corresponding time-lag, leading to lower increasing rate of average temperature and

liquid volume fraction, as well as diminishing the enhancement effects in the subsequent melting process. For the case of P=60 min, the liquid volume fraction exceeds 90% in the first half period, therefore, its large enhancement effects in the melting process can maintain in the later. From the whole melting process for all the cases, it is found that the difference of average temperature keeps decreasing between the small-period fluctuating heat sources and the large-period cases with the evolution of the melting process. That is because the heat is mainly stored by the sensible heat instead of latent heat in the later melting process for the large-period fluctuating heat source, therefore, the temperature difference inside the liquid PCM declines fast, making the average temperature approach with each other for these cases, as well as the liquid volume fraction of small-period fluctuating heat source approach the that of the large-period fluctuating heat source. The results demonstrated the importance of heat transfer enhancement for the late melting process of LTES under fluctuating heat source.

In addition to the melting rate, the energy storage capacity is another crucial indicator to evaluate the performance of LTES. From **Fig. 10** it can be seen that the total energy stored by PCM of all the fluctuating heat sources are smaller than that of the constant heat source. What's more, the total heat stored by PCM decreases with the increase of the fluctuating period. It is noticed that the total stored heat by PCM of small-period fluctuating heat sources is almost equal to that of the constant heat source, but the difference enlarges significantly when the fluctuating period increases to P=20 min. For the case of P=60 min, the largest difference in heat stored by PCM leads to about 9.5% smaller energy storage capacity in contrast to the constant heat source.

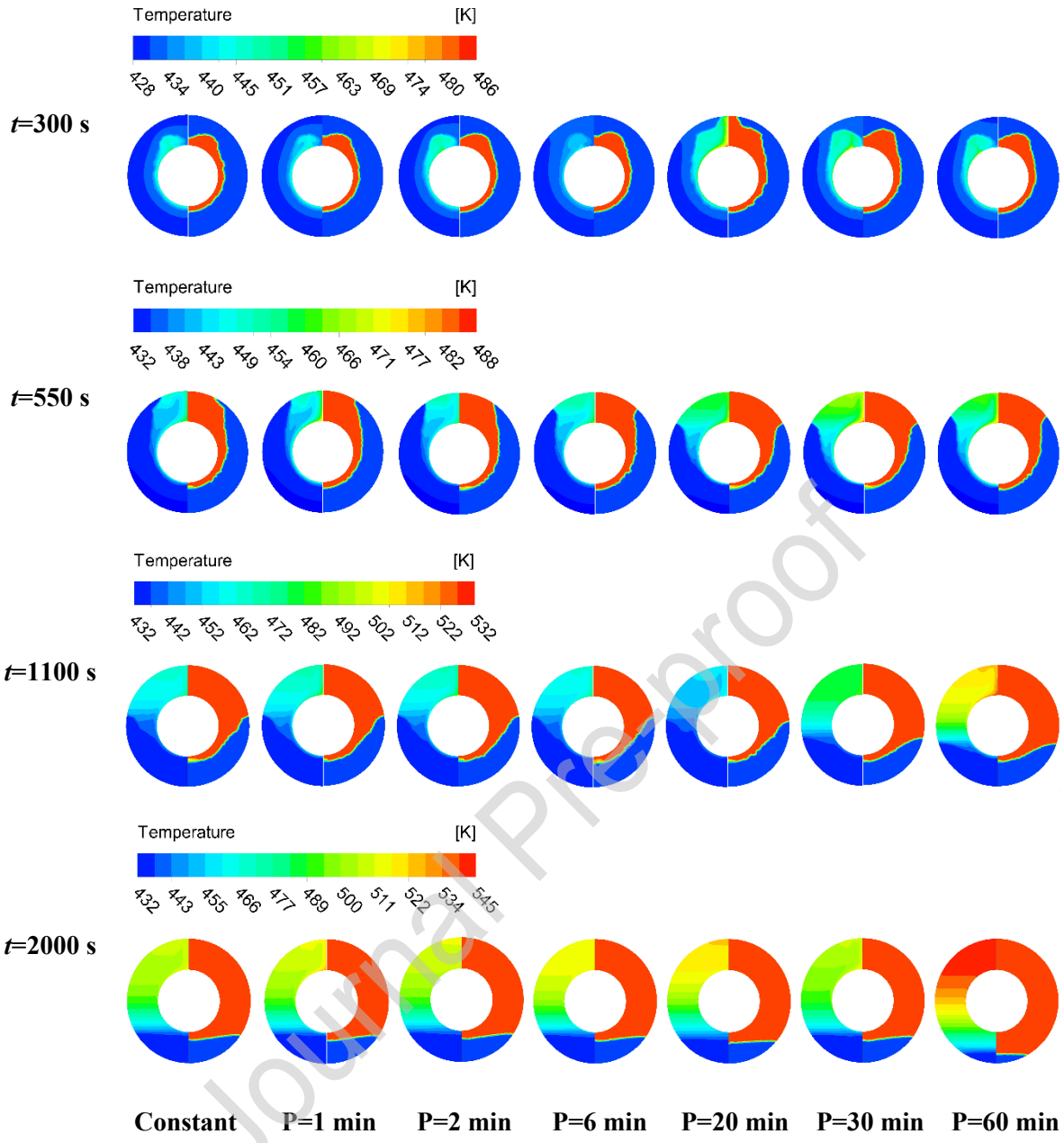

Fig. 9. The temperature contour and the liquid-solid interface at different moments. Left semicircle: temperature contour; Right semicircle: liquid-solid interface.

The reason is related to the temperature distribution during the melting process shown in **Fig. 9**. As is explained before, the small-period fluctuating (P= 1 min, 2 min, 6 min) heat sources lead to similar evolution of liquid volume fraction and temperature field to the constant heat source, i.e., the similar temperature difference during the heat transfer process between the HTF and PCM. For large-period

fluctuating heat sources (P= 20 min, 30 min, 60 min), the enhancement effects of melting process are larger with the increase of period compared to the constant heat source, as a consequence, the stage of sensible heat storage is faster to come, i.e., the higher average temperature and smaller temperature difference during the heat transfer process between the HTF and PCM.

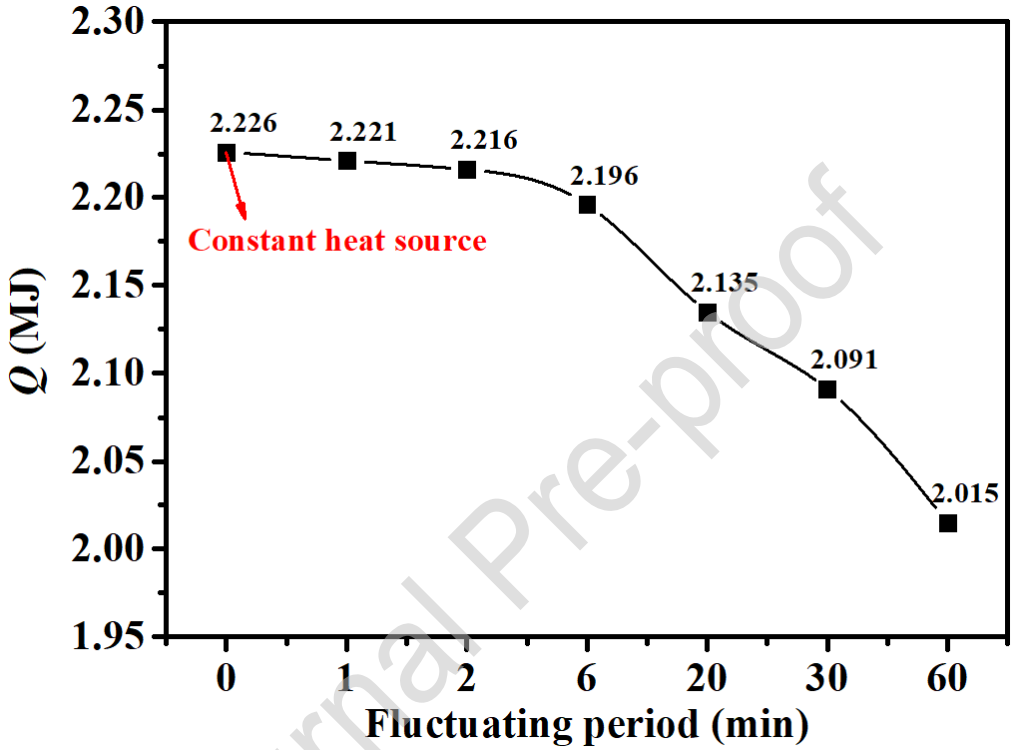

Fig. 10. The total energy stored by PCM under fluctuating heat sources with different period.

4.2 Effects of fluctuating amplitude

According to the previous analysis, only the larger fluctuating periods leads to significant enhancement effects on the heat transfer performance of LTES. In this section, the effects of different amplitudes of fluctuating heat sources are detailed investigated while their fluctuating periods are fixed as P=60 min. Comparing with the constant heat source, it is apparent in **Fig. 11** that all the fluctuating heat sources can accelerate the evolution of PCM liquid volume fraction and the

enhancement effect keeps improving when the fluctuating amplitude increases from 50 K to 150 K. For each fluctuating heat source, the enhancement effect is not evident at first and then continues to augment until the completion of the melting process in contrast to the constant heat source. The total melting for different heat sources is depicted in **Fig. 12**. Compared to the total melting time of the constant heat source (49.7 min), the total melting time for fluctuating heat sources dramatically decreases with the enlargement of fluctuating amplitude. It is 44.2 min for the case of A=50 K while the value is 32.3 min for the case of A=150 K, and they shorten the total melting time by 11.1% and 35.0%, respectively.

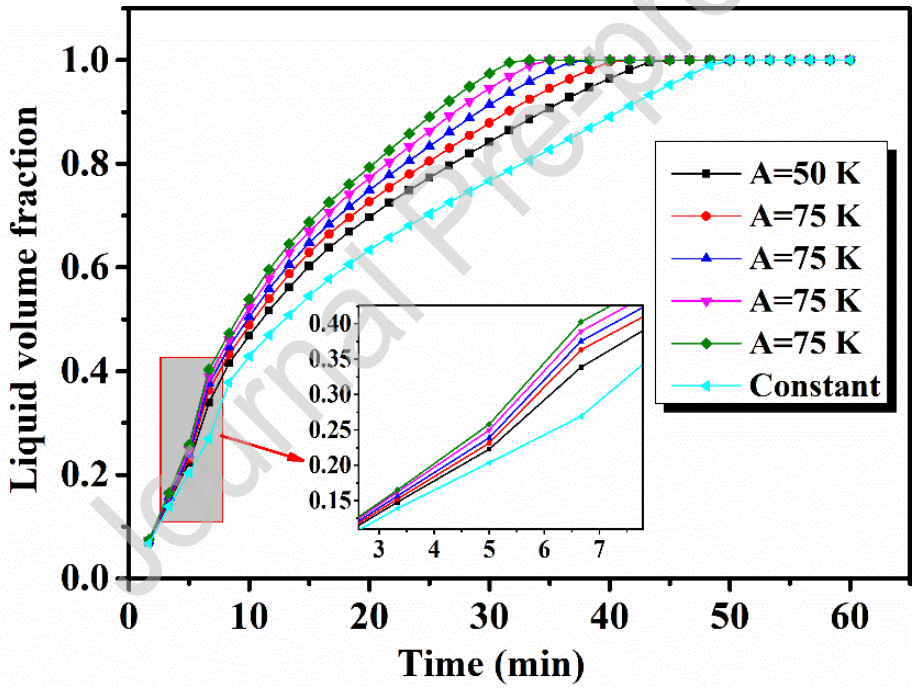

Fig. 11. The evolution of liquid volume fraction with melting time under different heat sources.

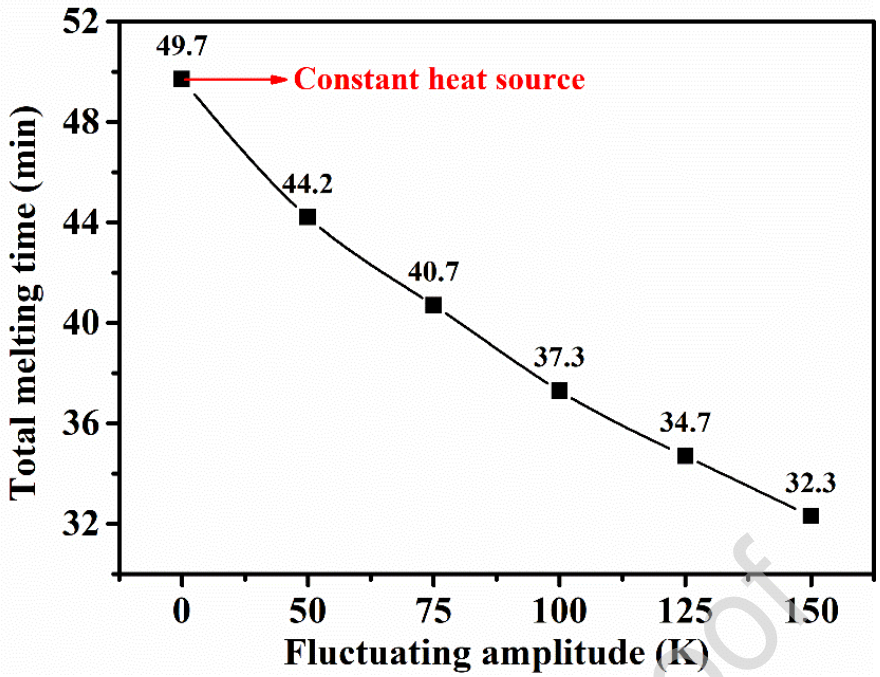

Fig. 12. The total melting time for fluctuating heat sources with different fluctuating heat sources

Based on the previous analysis, it can be understood that the effects of fluctuating amplitude are different from that of the fluctuating period. For the impacts of the fluctuating period, the large-period heat sources have significant enhancement effects on the heat transfer performance of LTES while the small-period fluctuating heat sources almost do not affect as previously explained. But all the heat sources with different amplitudes has evident enhancement effects on the heat transfer performance of LTES to a different extent. That is related to the melting process of LTES determined by the heat flux between the HTF and PCM. **Fig. 13** shows the comparison of timewise heat flux for a constant heat source and fluctuating heat sources with different fluctuating amplitude. For a constant heat source, the heat flux gradually decreases during the whole melting process because the increase of the PCM temperature leads to a continuously small temperature difference between the HTF and PCM. For each case of fluctuating heat source, the heat flux presents the wavelike characteristic just like the temperature variation of HTF. The timewise heat flux first increases due to the increase of HTF

temperature, then it decreases rapidly to the bottom because of the decline of HTF temperature and increase of PCM temperature, and later it turns to increase from the bottom owing to the rise of the HTF temperature.

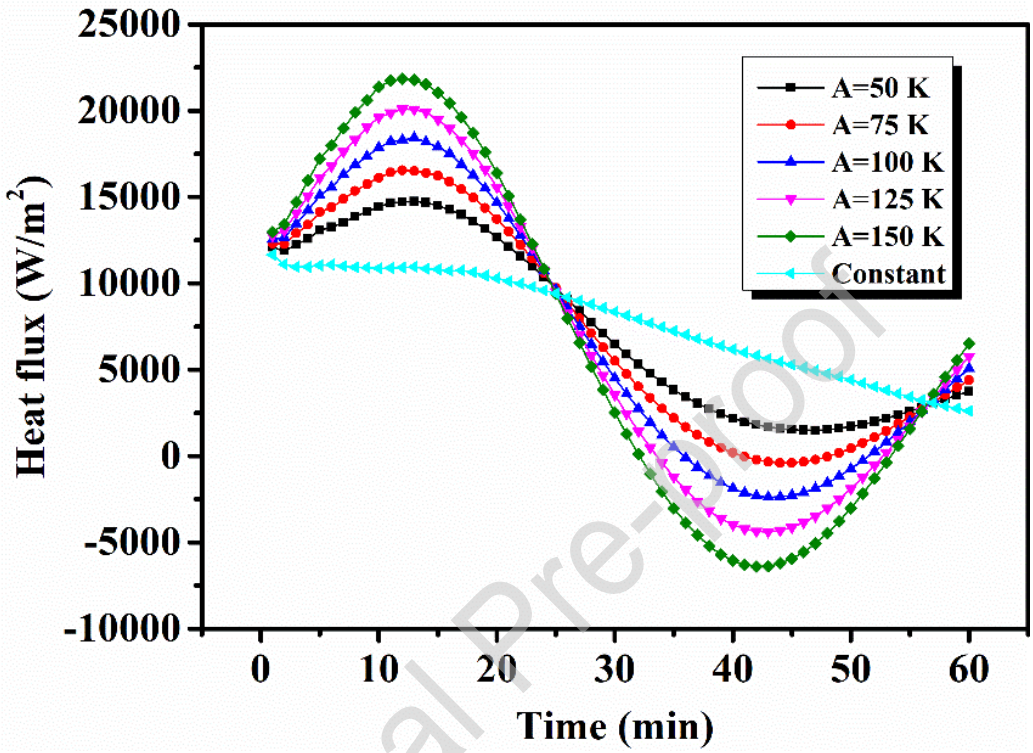

Fig. 13. The timewise heat flux for fluctuating heat sources with different fluctuating amplitude.

Taking the heat flux of constant heat source as the baseline, it can be found that the heat flux of fluctuating heat sources keeps larger some earlier before the moment of the first half period (about the moment of t=25 min), which is the reason to explain the fluctuating heat sources with different fluctuating amplitudes accelerate the melting process of LTES shown in **Fig. 11**. With the rising of the liquid volume fraction, the natural convection occurring in the liquid PCM enhances and it strengthens the heat transfer process between the PCM and HTF. Although the heat flux of fluctuating heat sources keeps smaller than that of the constant heat source during the second half period of the melting process, the natural convection can enhance the heat transfer process inside the PCM, which

weakens the adverse effects of the decline of heat flux on the heat transfer process.

To further illustrate the phenomenon, the temperature distribution (left semicircle) and solid-liquid interface (right semicircle) of PCM for different heat sources at different moments are presented in **Fig. 14**. Similar to the analysis of the effects of fluctuating periods, the results of constant heat source are taken as the comparison, and the moments at t=300 s, t=550 s, t=1100 s and t=2000 s are corresponding to the moments of liquid volume fraction f=0.2, f=0.4, f=0.6 and f=0.8 for constant heat source, respectively. At the moment of t=300 s, the enhancement effects on the temperature contour and liquid volume fraction are relatively insignificant compared to the constant heat source, since the difference in the heat flux between the constant and fluctuating heat source is small and the total amount of heat transferred to the PCM is small in this short time-lag. When the melting process reaches the moment of t=550 s, the liquid volume fraction and average temperature of PCM for constant heat source is significantly lower than that of fluctuating heat sources, furthermore, the fluctuating heat source with larger fluctuating amplitude results in apparently higher liquid volume fraction and average PCM temperature in contrast to that of the small-amplitude fluctuating heat sources. That is because the difference in the heat flux among all the fluctuating heat sources keeps enlarging with the increase of the fluctuating amplitude. The difference in the heat flux continues to increase before it attains the top and then it maintains a high level before the moment of t=20 min shown in **Fig. 13**, which can explain that the fluctuating heat sources bring about higher and higher average PCM temperature and liquid volume fraction comparing with the constant heat sources during the early stage (t<20 min) of the melting process, as well as the larger and larger difference in average PCM temperature and liquid volume fraction among the fluctuating heat sources. For example, at the

moment of t=1100 s, the maximum temperature differences between the constant heat source and the fluctuating case of A=50 K and A=150 K are 26 K and 89 K, respectively, while they are only 12 K and 31 K at the moment of t=550 s.

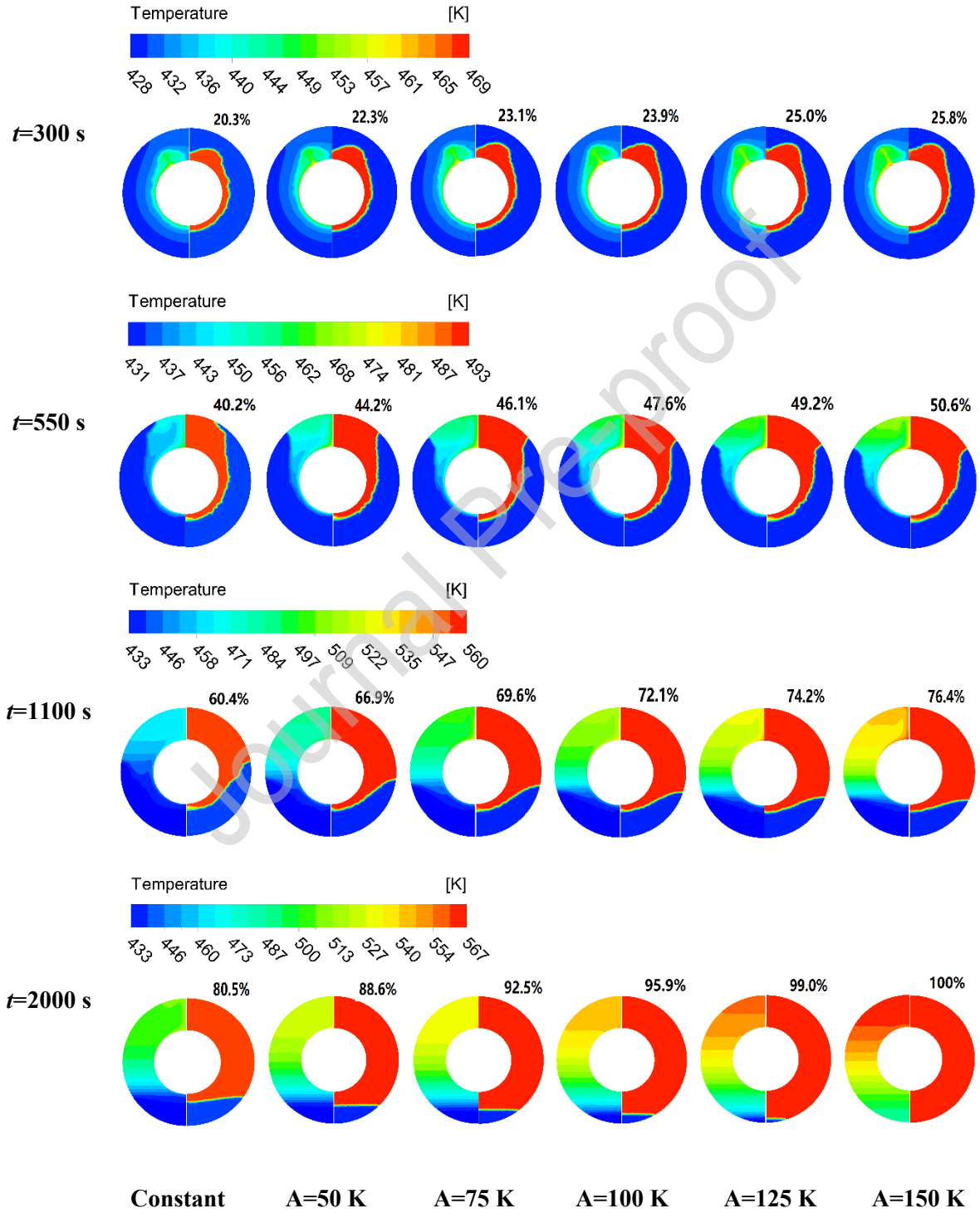

Fig. 14. The temperature contour and the liquid-solid interface at different moments. Left semicircle: temperature contour; Right semicircle: liquid-solid interface.

With the continuous evolution of melting process, the heat flux for a constant heat source is larger than that of all the fluctuating heat sources, and among all the fluctuating heat sources smaller fluctuating amplitude leads to a higher heat flux due to the sinusoidal variation of HTF temperature as shown in **Fig. 13**. In spite of the opposite variation trend of heat flux for constant and fluctuating heat sources, most of the PCM has melted at this time for each case and the thermal conduction is dominant instead of natural convection during the later stage of melting process, and the main energy storage mode is sensible energy storage of liquid PCM instead of latent heat storage of solid PCM, that is, the residual solid PCM at the bottom melts very slowly due to the low thermal conductivity of PCM, extending the total melting time of the melting process. For example, at the moment of t=2000 in **Fig. 14**, it can be found that the difference in average PCM temperature and liquid volume fraction among the constant heat source and fluctuating heat sources decreases with small extent compared to the previous moments, but the case of A=150 almost completes the melting process (f=1) while the constant case only attains f=0.8.

As for the energy storage capacity of LTES under different heat sources depicted in **Fig. 15**, it can be observed that LTES heated by the constant heat source obtains the maximum energy storage capacity. The energy storage capacity of fluctuating heat sources decreases with the rise of the fluctuating amplitude. The energy storage capacity for A=50 K and A=150 K is 4.5% and 28.5% smaller than that of constant heat source, respectively. The reason is related to the temperature distribution of PCM during the melting process shown in **Fig. 14**. In the first half period, the PCM temperature under

fluctuating heat sources increases rapidly due to the higher heat flux compared to the constant heat source, leading to the decline of the temperature difference between the HTF and PCM. In the second half period, the PCM temperature under fluctuating heat sources continues to increase but the HTF temperature is under the average temperature of HTF. Therefore, the PCM average temperature under fluctuating heat source keeps higher than that of constant heat source at any moments during the melting process, and the average PCM temperature improves with the rise of fluctuating heat source. However, the average temperature of HTF is fixed for all the heat sources in a period, that is, the lower temperature difference between the PCM and constant heat source achieves the maximum energy storage capacity, while the energy storage capacity decreases with the improvement of fluctuating amplitude for fluctuating heat sources.

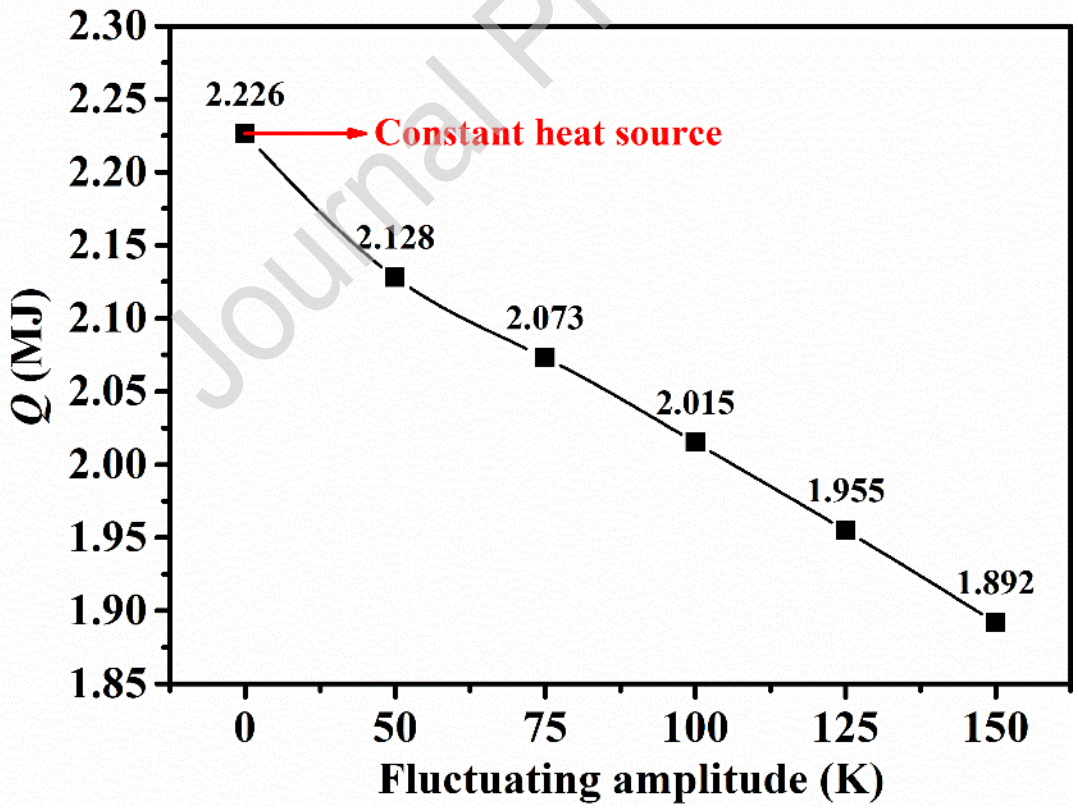

Fig. 15. The total energy stored by PCM under fluctuating heat sources with different amplitude.

4.3 Analysis of Stefan number

To evaluate the effects of different inlet temperature of HTF on the melting process pf LTES, the dimensionless Stefan number is used to describe the relationship of HTF temperature and melting temperature, and it is defined as the following formulation:

$$Ste = \frac{c_{p,p}\left(T_{av} - T_m\right)}{L} \tag{16}$$

According to the analysis of fluctuating period in Section 4.1, the fluctuating heat sources with small periods result in a similar melting process to the constant heat source. Therefore, the effects of the fluctuating period under different Stefan number are investigated in this section. **Fig. 16** shows the evolution of liquid volume fraction of LTES under fluctuating heat sources with different fluctuating period and Stefan number. For the certain *Ste* number, the fluctuating heat source with a larger period leads to faster melting process just like the analysed before. With the increase of *Ste* number, it can be observed that the evolution of liquid volume fraction of P=2 min is more closed to that of P=20 min and P=60 min, which indicates larger *Ste* number can motivate the enhancement effects of fluctuating heat source with P=2 min to a certain extent. That is because the larger *Ste* number means higher inlet temperature of HTF, resulting in larger heat flux and therefore larger liquid volume fraction in a corresponding period. Then the natural convection occurs earlier to enhance the heat transfer process in return and diminish the difference in melting rate between the case of P=2 min and cases with a larger period of P=20 min and 60 min.

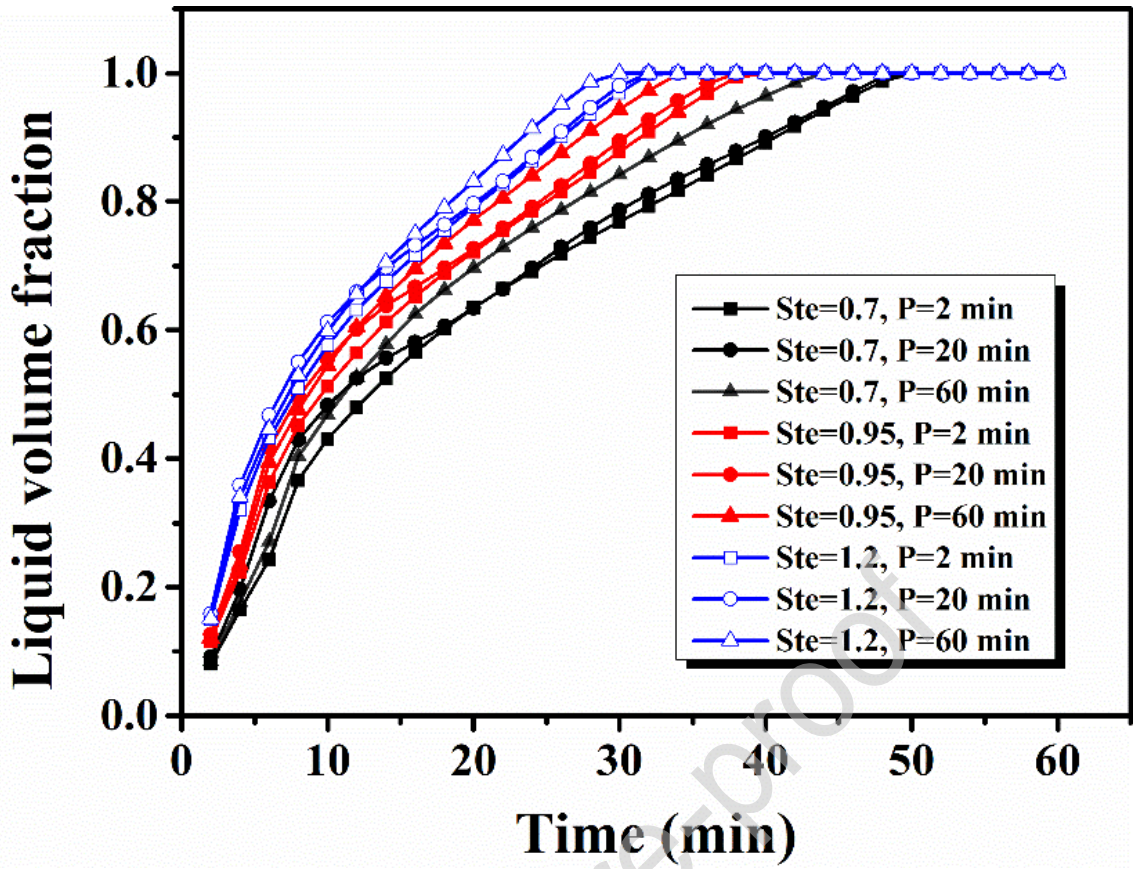

Fig. 16. The evolution of liquid volume fraction with melting time under different Stefan Number.

Fig. 17 indicates the corresponding total melting time for fluctuating heat sources under different *Ste* number. For any fixed period, the total melting declines in an increasing rate with the increase of *Ste* number because of the rise of average inlet temperature of HTF. However, the declining trend of total melting time is more rapid for a smaller-period fluctuating heat source. Besides, the difference in total melting between P=2 min and P=60 min decreases with the increase of *Ste* number. For example, the difference is 17.4 min between the P=2 min and P=60 min when the *Ste* number is equal to 0.7, while they are 17.1 min and 15 min for the case of *Ste*=0.95 and *Ste*=1.2, respectively. The total energy stored by PCM for each case is shown in **Fig. 18**. For any fixed *Ste* number, the case of P=2 min stores the maximum amount of heat during the whole melting process while the case of P=60 min ranks the last. For any fixed period, the energy storage capacity rises with the increase of *Ste* number.

It also can be found that the difference in energy storage capacity among these three cases enlarges with the increase of *Ste* number, which indicates the fluctuating heat source with smaller period can bring about larger energy storage capacity for LTES under the condition larger *Ste* number.

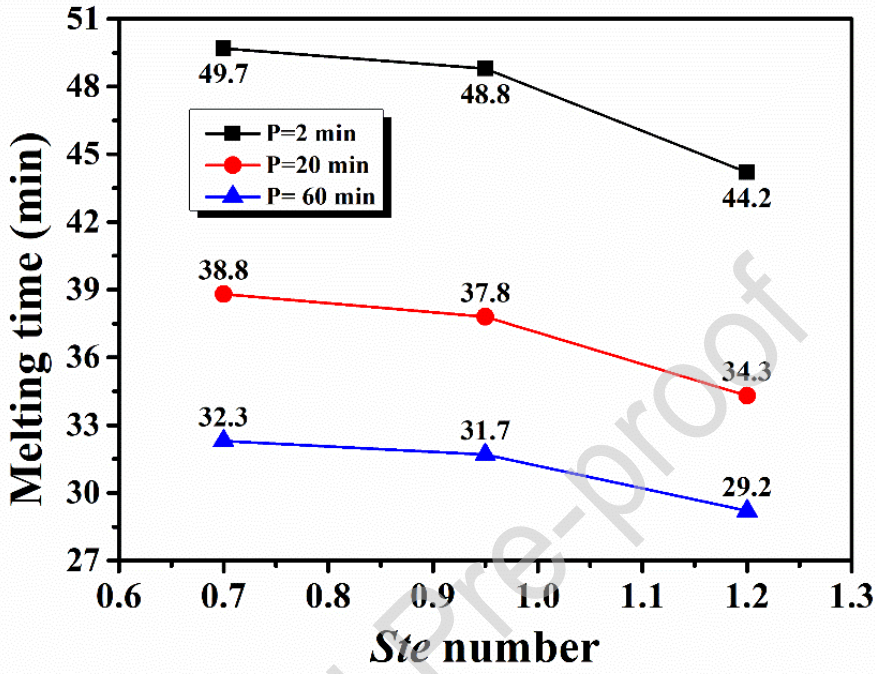

Fig. 17. The total melting time for fluctuating heat sources under different Stefan Number.

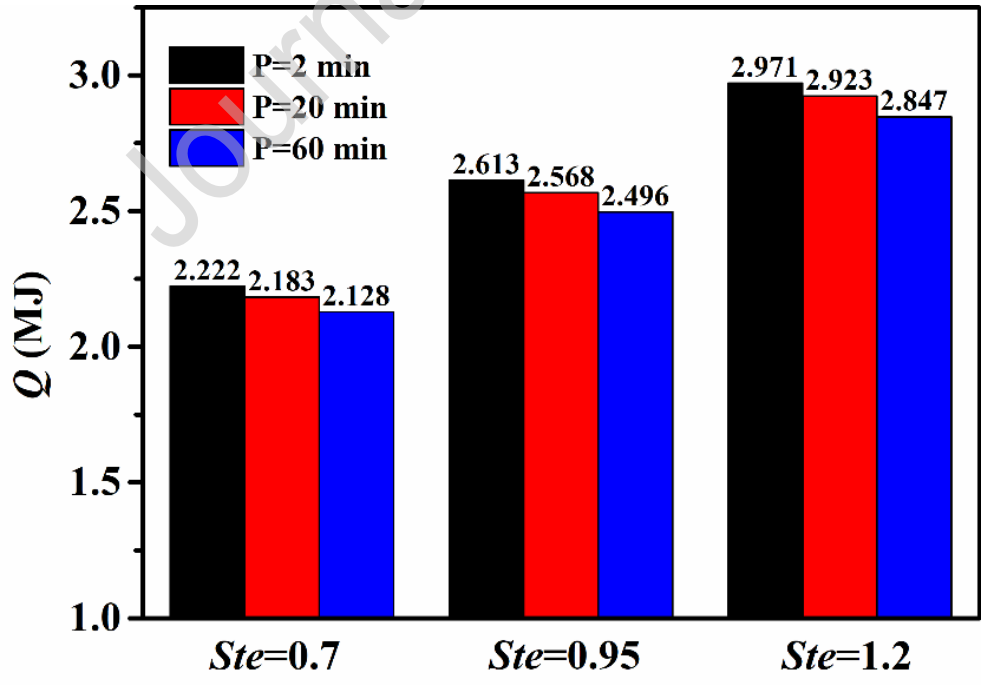

Fig. 18. The total energy stored by PCM under fluctuating heat sources with different *Ste* number.

5. Conclusions and prospects

In this study, the heat transfer performance of a shell-and-tube LTES heated by fluctuating heat source is analysed to overcome the barriers in waste heat recovery of fluctuating heat source. The effects of factors including period, amplitude and Stefan number of fluctuating heat source are detailed investigated. Some conclusions are drawn as follows

(1) Fluctuating heat sources with large period can significantly enhance the melting rate and shorten the total melting time, as well as lead to a smaller energy storage capacity of LTES compared to the constant heat source. While the fluctuating heat sources with small period has almost no effect on both the total melting time and energy storage capacity of LTES. For example, the total melting time and energy storage capacity for P=60 min are reduced 24.5% and 9.5% in contrast to that of constant heat source, but they almost the same for the case of P=1 min, 2 min and 6 min. The results indicate that the high-frequency fluctuation of fluctuating heat sources can be ignored when designing the LTES for heat recovery applications.

(2) Fluctuating heat sources with different amplitudes can substantially reduce the melting time and energy storage capacity of LTES in contrast to the constant heat source, furthermore, both the total melting time and energy storage capacity declines in a decreasing rate with the increase of fluctuating amplitude. In detail, compared with a constant heat source, the case of A=50 K and A=150 K reduce the total melting time and energy storage capacity by 11.1%, 35.0% and 4.4%, 15.0% respectively.

(3) Stefan number is used to evaluate the effects of different inlet temperature of HTF on the melting

process of LTES. The results illustrate that the fluctuating heat source with a larger period leads to faster melting process under a fixed Stefan number. But the total melting time of small-period fluctuating heat source gets more closed to that of a larger-period fluctuating heat source with the improvement of Stefan number.

(4) Fluctuating heat sources improve the melting rate of PCM, and therefore accelerate the melting process, but they lead to smaller energy storage capacity due to the inferior performance of temperature uniformity, that is, there is a discrepancy between the melting rate and energy storage capacity. In the future designing of LTES for fluctuating heat source, heat transfer enhancement technologies such as heat pipes should be explored to improve the temperature uniformity.

Although the effects of period and amplitude for fluctuating heat source on the heat transfer process of LTES is separately analysed in this study, the coupling effects of period and amplitude should be further investigated. In detail, map figures to illustrate the relationship of melting time and energy storage capacity with the period and amplitude of fluctuating heat source should be obtained. Besides, other important factors including the flowrate of fluctuating heat source, as well as the thermophysical properties of PCM, especially the thermal conductivity need to be carefully evaluated to reveal the comprehensive heat transfer mechanism of LTES under fluctuating heat source.

Acknowledgements

The research project has been funded bythe National Natural Science Foundation of China under grant number No. 51976176, No. 51806189. Supports from the China Science Foundation grant under 2018M640556, 2019T120514 and from Zhejiang Province Science Foundation under grant number

ZJ20180099 are highly acknowledged. The first author would like to thank the financial support from UK-China Joint Research and Innovation Partnership fund from Newton Fund providing the PhD scholarship under the grant number 201703780098.

Reference

[1] Li X, Tian H, Shu G, Hu C, Sun R, Li L. Effects of external perturbations on dynamic performance of carbon dioxide transcritical power cycles for truck engine waste heat recovery. Energy. 2018;163:920-31.

[2] Song J, Li X-s, Ren X-d, Gu C-w. Performance analysis and parametric optimization of supercritical carbon dioxide (S-CO2) cycle with bottoming Organic Rankine Cycle (ORC). Energy. 2018;143:406-16.

[3] Dal Magro F, Jimenez-Arreola M, Romagnoli A. Improving energy recovery efficiency by retrofitting a PCM-based technology to an ORC system operating under thermal power fluctuations. Applied Energy. 2017;208:972-85.

[4] Li X, Tian H, Shu G, Zhao M, Markides CN, Hu C. Potential of carbon dioxide transcritical power cycle waste-heat recovery systems for heavy-duty truck engines. Applied Energy. 2019;250:1581-99.

[5] Nardin G, Meneghetti A, Dal Magro F, Benedetti N. PCM-based energy recovery from electric arc furnaces. Applied Energy. 2014;136:947-55.

[6] Dal Magro F, Meneghetti A, Nardin G, Savino S. Enhancing energy recovery in the steel industry: Matching continuous charge with off-gas variability smoothing. Energy Conversion and Management. 2015;104:78-89.

[7] Liu G, Liu J, E J, Li Y, Zhang Z, Chen J, et al. Effects of different sizes and dispatch strategies of thermal energy storage on solar energy usage ability of solar thermal power plant. Applied Thermal Engineering. 2019;156:14-22.

[8] Jafari Mosleh H, Ahmadi R. Linear parabolic trough solar power plant assisted with latent thermal energy storage system: A dynamic simulation. Applied Thermal Engineering. 2019;161:114204.

[9] Li S, Ma H, Li W. Dynamic performance analysis of solar organic Rankine cycle with thermal energy storage. Applied Thermal Engineering. 2018;129:155-64.

[10] Freeman J, Guarracino I, Kalogirou SA, Markides CN. A small-scale solar organic Rankine cycle combined heat and power system with integrated thermal energy storage. Applied Thermal Engineering. 2017;127:1543-54.

[11] Dal Magro F, Savino S, Meneghetti A, Nardin G. Coupling waste heat extraction by phase change materials with superheated steam generation in the steel industry. Energy. 2017;137:1107-18.

[12] Yu X, Li Z, Lu Y, Huang R, Roskilly AP. Investigation of organic Rankine cycle integrated with double latent thermal energy storage for engine waste heat recovery. Energy. 2019;170:1098-112.

[13] Xu ZY, Wang RZ, Yang C. Perspectives for low-temperature waste heat recovery. Energy. 2019;176:1037-43.

[14] Guo C, Zhang W. Numerical simulation and parametric study on new type of high temperature latent heat thermal energy storage system. Energy Conversion and Management. 2008;49(5):919-27.

[15] Wang W-W, Zhang K, Wang L-B, He Y-L. Numerical study of the heat charging and discharging characteristics of a shell-and-tube phase change heat storage unit. Applied Thermal Engineering. 2013;58(1):542-53.

[16] Tao YB, Carey VP. Effects of PCM thermophysical properties on thermal storage performance of a shell-and-tube latent heat storage unit. Applied Energy. 2016;179:203-10.

[17] Agyenim F, Eames P, Smyth M. A comparison of heat transfer enhancement in a medium temperature thermal energy storage heat exchanger using fins. Solar Energy. 2009;83(9):1509-20.

[18] Wang P, Yao H, Lan Z, Peng Z, Huang Y, Ding Y. Numerical investigation of PCM melting process in sleeve tube with internal fins. Energy Conversion and Management. 2016;110:428-35.

[19] Ebrahimi A, Hosseini MJ, Ranjbar AA, Rahimi M, Bahrampoury R. Melting process investigation of phase change materials in a shell and tube heat exchanger enhanced with heat pipe. Renewable Energy. 2019;138:378-94.

[20] Das N, Takata Y, Kohno M, Harish S. Effect of carbon nano inclusion dimensionality on the melting of phase change nanocomposites in vertical shell-tube thermal energy storage unit. International Journal of Heat and Mass Transfer. 2017;113:423-31.

[21] Yang X, Yu J, Guo Z, Jin L, He Y-L. Role of porous metal foam on the heat transfer enhancement for a thermal energy storage tube. Applied Energy. 2019;239:142-56.

[22] Tao YB, He YL, Liu YK, Tao WQ. Performance optimization of two-stage latent heat storage unit based on entransy theory. International Journal of Heat and Mass Transfer. 2014;77:695-703.

[23] Fang Y, Niu J, Deng S. An analytical technique for the optimal designs of tube-in-tank thermal energy storage systems using PCM. International Journal of Heat and Mass Transfer. 2019;128:849-59.

[24] Deng S, Nie C, Jiang H, Ye W-B. Evaluation and optimization of thermal performance for a finned double tube latent heat thermal energy storage. International Journal of Heat and Mass Transfer. 2019;130:532-44.

[25] Tao YB, He YL. Numerical study on thermal energy storage performance of phase change material under non-steady-state inlet boundary. Applied Energy. 2011;88(11):4172-9.

[26] Elbahjaoui R, El Qarnia H. Numerical Study of a Shell-and-Tube Latent Thermal Energy Storage Unit Heated by Laminar Pulsed Fluid Flow. Heat Transfer Engineering. 2017;38(17):1466-80.

[27] Xu HJ, Zhao CY. Thermal performance of cascaded thermal storage with phase-change materials

(PCMs). Part II: Unsteady cases. International Journal of Heat and Mass Transfer. 2017;106:945-57.

[28] Huo Y, Zong J, Rao Z. The investigations on the heat transfer in thermal energy storage with time-dependent heat flux for power plants. Energy. 2019;175:1209-21.

[29] Jiménez-Arreola M, Pili R, Dal Magro F, Wieland C, Rajoo S, Romagnoli A. Thermal power fluctuations in waste heat to power systems: An overview on the challenges and current solutions. Applied Thermal Engineering. 2018;134:576-84.

[30] Pereira da Cunha J, Eames P. Thermal energy storage for low and medium temperature applications using phase change materials – A review. Applied Energy. 2016;177:227-38.

[31] Tao YB, He YL. Effects of natural convection on latent heat storage performance of salt in a horizontal concentric tube. Applied Energy. 2015;143:38-46.

[32] Al-Abidi AA, Mat S, Sopian K, Sulaiman MY, Mohammad AT. Numerical study of PCM solidification in a triplex tube heat exchanger with internal and external fins. International Journal of Heat and Mass Transfer. 2013;61:684-95.

[33] Deng S, Nie C, Wei G, Ye W-B. Improving the melting performance of a horizontal shell-tube latent-heat thermal energy storage unit using local enhanced finned tube. Energy and Buildings. 2019;183:161-73.

[34] Lacroix M. Numerical simulation of a shell-and-tube latent heat thermal energy storage unit. Solar Energy. 1993;50(4):11.

Durham University

Department of Engineering

South Road
Durham DH1 3LE
United Kingdom

10th - February - 2020

Dear Editor and Reviewers of ***Energy***,

Conflict of interest statement

On behalf of all the co-authors of the submitted paper, I can confirm that we have no financial and personal relationships with other people or organizations that can inappropriately influence our work, there is no professional or other personal interest of any nature or kind in any product, service and/or company that could be construed as influencing the position presented in, or the review of, the manuscript entitled, '**Effects of fluctuating thermal sources on a shell-and-tube latent thermal energy storage during charging process**'.

Yours Faithfully,

Dr Yiji Lu, *BEng (Hons), Mphil, PhD*

Assistant Professor (Research) in the Department of Engineering
Fellow in the Durham Energy Institute
Web: https://www.dur.ac.uk/research/directory/staff/?mode=staff&id=19000

Durham University is a world top 100 university
Ranked 5th in The Guardian University Guide 2019
Ranked 7th in The Times and The Sunday Times Good University Guide 2019

Durham University Department of Engineering

Durham University Durham Energy Institute

Associate Editor: Frontiers in Energy Research (ISSN 2296-598X)
Guest Editor: Energies (ISSN 1996-1073)
Editorial Board Member: 'Energy Reports' (ISSN 2352-4847 - Elsevier), 'Scientific Reports' (ISSN 2045-2322 – Nature), 'Thermal Science and Engineering Progress' (ISSN: 2451-9049 – Elsevier), 'Frontiers in Energy Research' (ISSN 2296-598X), 'International Journal of Energy and Power Engineering', 'Current Analysis on Energy and Environmental Sciences'
Member of the EPSRC Associate Peer Review College

nature research Editorial Board Member for Scientific Reports

ELSEVIER Editorial Board Member for Energy Reports

Research Gate: https://www.researchgate.net/profile/Yiji_Lu
Mendeley: https://www.mendeley.com/profiles/dr-yiji-lu/
ORCID: https://orcid.org/0000-0001-5552-3894
Publons: https://publons.com/researcher/3147656/yiji-lu/
Google Scholar: https://scholar.google.co.uk/citations?user=T0OoMcEAAAAJ&hl=en

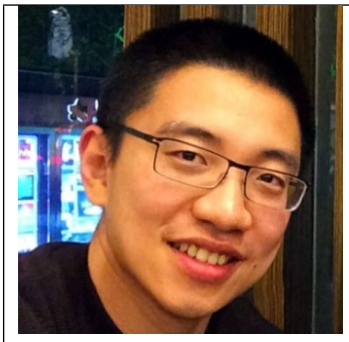

Short Biography of the corresponding author

Dr. Yiji Lu is an Assistant Professor (Research) of Energy Systems in the Department of Engineering and Fellow in the Durham Energy Institute at Durham University, with research focuses on Renewable and Clean Energy Conversion, Energy Storage and Cleaner/Alternative Fuels to tackle Climate Change Challenges. Dr Lu obtained PhD from Newcastle University in 2016 and was awarded a prestigious **Chinese Government Award** from the China Scholarship Council for his PhD study in May 2016 by the Chinese Ambassador to the UK. Dr Lu has a strong track record of high-quality research in energy conversion systems having published over 60 articles in high-quality international journals and peer-reviewed conferences, and one book chapter with over 400 citations and an H-index of 12 and i10-index of 16 (Google Scholar). Elsevier gave him several **outstanding reviewer awards** in October 2016 (Applied Thermal Engineering), January 2017 (Applied Energy) and May 2017 (Energy). He was an invited session chair at the 9th International Conference on Applied Energy, Cardiff, UK, 10th International Conference on Applied Energy, Hong Kong, China and 11th International Conference on Applied Energy, Västerås, Sweden, which is the largest international conference organised by Elsevier's prestigious Applied Energy (Impact Factor 7.900). Since 2018, Dr Lu serves as a Guest Editor of the international journal 'Energies' (Impact Factor 2.676) and is an Associate Editor of the international journal Frontiers in Energy Research' (Impact Factor 1.52). Dr Lu is now serving as the editorial board member in an Elsevier Journal '**Energy Reports**' ISSN 2352-4847 and a **Nature Research Journal** '**Scientific Reports**' ISSN 2045-2322.

Credit author statement for 'Effects of fluctuating thermal sources on a shell-and-tube latent thermal energy storage during charging process'

Zhi Li: Writing- Original draft preparation, Formal analysis, Software,

Xiaoli Yu: Conceptualization, Supervision, Methodology

Lei Wang: Methodology, Data curation, Funding acquisition

Yiji Lu: Conceptualization, Writing- Reviewing and Editing, Supervision

Rui Huang: Supervision, Funding acquisition, Project administration

Jinwei Chang: Investigation, Writing- Original draft preparation, Visualization

Ruicheng Jiang: Data curation, Investigation, Software, Formal analysis